

Receive

DE90 002989

NOV 2

Submitted to the AIAA 16th Aerodynamic Ground Testing Conference  
June 18-20, 1990  
Seattle, Washington

Slotted-Wall Research with Disk and Parachute Models  
in a Low-Speed Wind Tunnel\*

by

J. M. Macha, R. J. Buffington and J. F. Henfling  
Sandia National Laboratories  
Albuquerque, New Mexico

and

D. Van Every and J. L. Harris  
DSMA International, Inc.  
Mississauga, Ontario

Introduction

Bluff bodies in general, and parachutes in particular, often require large blockage corrections when tested in conventional solid-wall wind tunnels. The semi-empirical correction method developed by Maskell<sup>1</sup> has been successfully applied to a variety of rigid shapes whose aerodynamics are dominated by a region of separated flow. In a recent study,<sup>2</sup> this method was extended to flexible, cloth parachutes of standard design. According to experimental data reported in Reference 2, the uncorrected drag coefficient of a parachute presenting a 10% geometric blockage (i.e., the ratio of frontal projected area of the inflated model to the cross-sectional area of the test section) can be in error by up to 30%. Comparatively, the required  $C_D$ -correction for a streamlined model with the same projected area may be only 5%. While the Maskell-type method was shown to accurately correct parachute drag and base-pressure coefficients at geometric blockages as high as 22%, there are occasions when it is desirable to reduce the

\*. This research was partly funded by the U. S. Department of Energy under contract number DE-AC04-76DP00789.

## **DISCLAIMER**

**This report was prepared as an account of work sponsored by an agency of the United States Government. Neither the United States Government nor any agency thereof, nor any of their employees, makes any warranty, express or implied, or assumes any legal liability or responsibility for the accuracy, completeness, or usefulness of any information, apparatus, product, or process disclosed, or represents that its use would not infringe privately owned rights. Reference herein to any specific commercial product, process, or service by trade name, trademark, manufacturer, or otherwise does not necessarily constitute or imply its endorsement, recommendation, or favoring by the United States Government or any agency thereof. The views and opinions of authors expressed herein do not necessarily state or reflect those of the United States Government or any agency thereof.**

---

## **DISCLAIMER**

**Portions of this document may be illegible in electronic image products. Images are produced from the best available original document.**

severity of test-section boundary effects. A notable example is the measurement of the pressure distribution over both the attached- and separated-flow regions of the canopy. Because the wall-induced interference velocity varies over the length of a model, local pressure coefficients require corrections based on local flow conditions if the boundary effect is large. Maskell's method provides only an average correction to the flow in the vicinity of the model. Furthermore, the empirical factor derived in Reference 2 for the Maskell equation may not be appropriate for some types of parachutes. If parachutes could be tested under boundary effects less-severe than those imposed by solid walls, then less correction would be required and less accuracy could be tolerated from whatever correction method is used.

The possibility of using ventilated walls to minimize boundary interference derives from the earliest theoretical studies comparing solid-wall to open-jet test sections.<sup>3</sup> Many of the interference effects are of opposite sign for these two extreme geometries; hence, by using a partially-open tunnel it is possible to reduce, or even eliminate, some aspects of boundary interference. Reference 4 gives a comprehensive summary of the theoretical treatment of subsonic wall interference for both slotted and perforated walls. The subsequent development of transonic test sections using ventilated walls for both Mach number control and shock wave cancellation has continued to encourage the pursuit of a general theory of the ventilated-wall boundary condition.<sup>5,6</sup>

In the past, slotted-wall research has dealt almost exclusively with streamlined rather than bluff wind tunnel models. One exception is the testing of road vehicles which in some cases can be classified as semi-bluff shapes.<sup>7</sup> This situation exists because streamlined shapes make up the bulk of testing activity and because a bluff shape is inherently more difficult to analyze even in the absence of tunnel walls. Therefore, practical information about the effects of slotted walls on the measured aerodynamic characteristics of parachutes can be found only by direct experiment. In the case of conventional, nonlifting parachutes, lift-interference is not a factor; only the blockage interference, which stems from the velocity increment and gradient in the vicinity of the model, need be considered.

### Scope of the Research

The primary factors which determine the nature and degree of slotted-wall interference are the geometric blockage ratio (GBR), the wall open area ratio (OAR), and, in the case of a finite-length test section, the location of the model with respect to the upstream beginning of the slots. All of these factors were systematically varied using a set of rigid, metal disk models and a set of flexible, cloth parachute models. Four different-size disks provided GBR's of 0.020, 0.050, 0.100 and 0.150. The three geometrically similar parachutes were sized to provide nominal GBR's of 0.05, 0.10 and 0.15 based on the inflated frontal area. The tests were conducted in the DSMA International, Inc. low speed wind tunnel, with a 2.36ft x 2.36ft x 6.56ft-long test section. The OAR was set to 0.00, 0.10, 0.20, or 0.30 by fitting appropriate solid panels to a framework around the square test section. The ventilated-wall configurations consisted of five solid slats separated by four open slots of constant width, on each of the four walls. The test section was surrounded by an "infinite-volume" plenum consisting of the high-bay room housing the wind tunnel circuit. The nominal corrected dynamic pressure was 10 psf, yielding corrected Reynolds numbers based on model diameter of  $2.4 \times 10^5$  -  $6.5 \times 10^5$ .

The disk models were supported from behind, on the centerline of the test section, by a sting containing a six-component strain-gage balance to measure the aerodynamic loads (see Fig. 1). For the parachute models, the sting projected through the canopy vent and was attached to the confluence point of the suspension lines as shown in Fig. 2. Prior to conducting the slotted-wall investigation, all of the models were tested in the Lockheed-Georgia 16ft x 23ft wind tunnel using the same sting/balance assembly to obtain interference-free loads data. Great importance was placed on the accurate measurement of air speed and model drag. The propagation of uncertainties in the calculation of model drag coefficient from these measurements was estimated using the method of Kline and McClintock (see, e.g., Ref. 8). For the smallest model (i.e., GBR = 0.02), the worst case uncertainty in  $C_D$  is  $\pm 2\%$ ; for the largest models (GBR = 0.15), the uncertainty is less than  $\pm 1\%$ .

The thin, sharp-edged disks made possible an investigation of wall interference for a bluff, axisymmetric shape under steady-flow conditions without the subtle geometric variability that often occurs over time with cloth parachute models. On the other hand, routine testing of parachutes in wind tunnels often includes measuring the time-dependent drag while the parachute inflates.<sup>9</sup> During the inflation, the GBR increases rapidly from near zero to the fully inflated value. More importantly, the drag reaches a peak that may be twice the fully inflated steady-flow value because of the effect of the added mass of the air. In Reference 2, it was shown that the severity of steady-flow, solid-wall interference was directly proportional to parachute drag area (i.e.,  $D/q$ ). The results of the present investigation provide, for the first time, quantitative information on the character of wall-interference for both solid and slotted walls during the transient inflation process. The inflation-test procedure consisted of securing the collapsed parachute around the sting using a length of Kevlar cord and a slip knot (see Fig. 3). With the airstream at the desired condition, the inflation was initiated by pulling the end of the cord and releasing the knot. A related concern is the effect of the increase in model drag on airstream properties. Using fast-response instrumentation, the time-dependent test-section dynamic and total pressures were measured and have been correlated with the parachute drag.

#### Representative Results and Discussion

With slotted walls, fluid displaced by the model wake remains outside the finite-length test section. Some means must be used to direct this fluid into the diffuser without creating a streamwise static pressure gradient in the test section that might significantly affect drag measurements. In the present test, the reentry section consisted of adjustable flaps at the mouth of the diffuser as shown in Fig. 4. If the flap setting  $\delta_f$  is too small for a given size model and wake, a negative pressure gradient will exist in the aft portion of the test section; conversely, setting  $\delta_f$  too large will induce a positive pressure gradient. A flagrantly incorrect flap setting will shorten the usable length of the test section. For each slotted-wall OAR, the sensitivity of model  $C_D$  to

flap setting and model location was experimentally determined using the 0.1-GBR disk.

The results of this sensitivity study for the 0.3-OAR wall are shown in Fig. 5. The drag coefficient of the 0.1-GBR disk, uncorrected for wall-interference, is plotted as a function of nondimensional distance from the upstream end of the test section,  $X$ , and flap setting,  $\delta_f$ . ( $X = x/\sqrt{C}$ , where  $C$  is the cross-sectional area of the test section.) The downstream end of the test section is at  $X = 2.78$ . The curves illustrate that the negative pressure gradient associated with the smallest flap setting of 1 in. causes a significant increase in  $C_D$  as far forward as the middle of the test section. On the other hand,  $C_D$  is insensitive to  $\delta_f$  for  $3 \text{ in.} \leq \delta_f \leq 5 \text{ in.}$  as far aft as  $X = 1.73$ . Based on these results for the 0.10-GBR disk, it was decided to set  $\delta_f = 4$  in. for the rest of the models tested and to conservatively take  $X = 1.39$  as the aft-most model location for measurements to be reasonably unaffected by the downstream boundary condition.

Figure 5 also illustrates that a considerable length at the beginning of the test section is required for the full effect of the slots to be realized; i.e.,  $C_D$  asymptotically approaches a value that is independent of the upstream boundary condition. For a given size model, this development length increases as the wall OAR decreases. This trend is demonstrated in Fig. 6 for the 0.1-GBR disk. As a reference, the drag coefficient measured with the solid walls is included in the plot. For OAR's of 0.2 and 0.3, there is only a small interval in the middle of the test section where the model is unaffected by either the upstream or downstream boundaries. In the case of the wall OAR of 0.1, the test section is not long enough to achieve the full benefit of the slots. Examination of the data for all of the disk models shows that there is a positive correlation between the development length and the geometric blockage ratio.

Also shown in Fig. 6 is the interference-free value of  $C_D$  as measured in the large, Lockheed-Georgia wind tunnel. Consistent with previous analyses and experiments using more streamlined shapes reported in the literature, the interference effect on  $C_D$  is opposite in sign for the solid and slotted walls. Moreover, the magnitude of the required correction is

smaller by a factor of at least five for the slotted walls. Although no confirming data are available, it is conjectured that the degree of interference observed with the 0.3-OAR wall is very near to that which would occur in a completely open-jet test section of the same dimensions.

A summary of the combined effects of wall OAR and model GBR is presented in Fig. 7. Here, the drag coefficient for each disk model has been normalized by the respective interference-free drag coefficient,  $C_{D,\infty}$ . The data shown are for a model location of  $X = 1.39$  (i.e., at the center of the test section). Based on the observed trends with model location discussed earlier, the drag coefficients for the two largest models in the 0.1-OAR walls are influenced by both the upstream and downstream boundary conditions. If the test section had been long enough to allow full development of the slotted-wall flow for this OAR, those two drag coefficients would probably be slightly smaller than the interference-free value.

As stated earlier, testing parachutes in wind tunnels often involves measuring the time-dependent loads as the canopy inflates in a constant-speed airstream. Accurate determination of the peak drag is critical to the structural design of a parachute as well as predicting its deceleration performance under actual flight conditions. There are no previous data on the nature of wall interference during the transient inflation process. In the present investigation, the three model parachutes with nominal GBR's of 0.05, 0.10 and 0.15 were allowed to inflate in the presence of each of the four wall configurations. The parachutes were tested with the leading edge of the inflated canopy at the middle of the test section,  $X = 1.39$ . As with the disk models, interference-free drag data had been obtained previously in the Lockheed-Georgia wind tunnel.

It was anticipated that the increase in model drag during inflation would result in a velocity decrease in the tunnel circuit. If the decrease was large and dependent on the test section wall geometry, then the desired interference data might be obscured. To minimize this possibility, screens were added between the diffuser and fan sections to increase the circuit losses and make the effect of the model less apparent. Total and dynamic

pressures at the entrance to the test section were measured using low-volume transducers that were close-coupled to a wall static orifice and a pitot tube. Table 1 shows the eventual percent drop in test section dynamic pressure for each of the models and wall configurations. Within measurement accuracy, the change in airstream properties is independent of wall OAR for the two smallest models; for the 0.15-GBR model the drop in dynamic pressure decreases slightly as the wall OAR increases. The dynamic aspects of these changes in test section conditions during the inflation transient are discussed in the following paragraphs.

Table 1. Decrease in Dynamic Pressure  
with Parachute Inflation

GBR	OAR	$(\Delta q/q) \times 100$
.05	0.0	-1.01
	0.1	-1.25
	0.2	-1.19
	0.3	-1.32
.10	0.0	-2.75
	0.1	-3.12
	0.2	-2.77
	0.3	-2.68
.15	0.0	-6.35
	0.1	-6.25
	0.2	-5.75
	0.3	-4.93

Figure 8 displays the direct instrument outputs for the 0.15-GBR parachute inflating in the presence of the solid walls. The decrease in test section dynamic pressure occurs simultaneously with the increase in model drag. At the instant when the peak drag is reached, the dynamic pressure has realized approximately one-half of its eventual decrease. The lowest trace shows that test section total pressure increases during the inflation, and examination of the reduced data indicates a significant increase in static pressure of  $\Delta p_s/q = 0.33$ . It is obvious that a transient static pressure gradient must exist in the test section during the inflation, producing an undetermined horizontal buoyancy force on the model.

Figure 9 presents results for the same model, but with the 0.2-OAR slotted walls. One effect of the ventilated test section is to delay the decrease in dynamic pressure until after the parachute has completely inflated. Furthermore, contrary to the solid-wall situation and consistent with the constant static-pressure environment provided by the surrounding plenum, total pressure also decreases.

A quantitative assessment of the influence of the test section walls on the inflation event can be made by examining the peak drag as a function of model size and wall OAR. Since the frontal projected areas of the inflated parachutes are not precisely known, the GBR is replaced by an "aerodynamic" blockage ratio based on the steady-flow, interference-free drag area; i.e.,  $ABR = (C_D S)_\infty / C$ . In Figure 10, the maximum value of the drag coefficient normalized by the peak interference-free value is plotted as a function of ABR and wall OAR. Each of the symbols in the figure represents the average of several repeated inflations. The observed scatter in the data for a given model and wall configuration caused by the random nature of the inflation process is approximately  $\pm 6\%$ . There is no discernible wall-interference effect for any of the slotted-wall configurations, even with the largest model. The data marginally suggest a positive correlation between the peak  $C_D$  and model size for the solid wall. It is unclear whether this behavior is a direct result of wall interference or a consequence of the transient static pressure gradient discussed earlier.

#### Summary and Conclusions

An experimental investigation of slotted-wall blockage interference has been conducted using disk and parachute models in a low speed wind tunnel. Test section open area ratio, model geometric blockage ratio, and model location along the length of the test section were systematically varied. Resulting drag coefficients were compared to each other and to interference-free measurements obtained in a much larger wind tunnel where the geometric blockage ratio was less than 0.0025.

The steady-flow disk data provide new insight into the nature of slotted-wall interference for axisymmetric or other low-aspect ratio bluff shapes. Specifically, the test results support the following conclusions.

1. The geometry of the displaced-flow reentry device at the downstream end of the test section could significantly influence model drag as far forward as the middle of the test section.
2. The full benefit of the slots was achieved asymptotically as the model was moved downstream from the leading edge of the slots, and this flow development length increased with decreasing wall OAR and increasing model size.
3. For the test section used (i.e., length =  $2.78/C$ ), full benefit of the slots was not achieved for the two largest disk models with the 0.1-OAR walls.
4. The interference effect on drag coefficient was opposite in sign for the slotted and solid walls, and the magnitude of the required correction was smaller by a factor of at least five with the slotted walls. Up to a GBR of 0.05, the degree of interference with the slotted walls was independent of OAR within the accuracy of the measurements.

The experiments with the parachute models have provided the first quantitative information on tunnel circuit response and wall interference during the transient inflation process. The following conclusions are offered.

5. In the case of the solid walls, test section dynamic pressure decreased and total pressure increased during the inflation process. It is conjectured that the resulting increase in static pressure at the measurement location was accompanied by a transient static pressure gradient in the test section that produced a horizontal buoyancy force of undetermined magnitude.

6. With the slotted walls, the decrease in dynamic pressure occurred after the parachute was completely inflated. A concurrent decrease in total pressure confirmed that the static pressure in the test section remained constant and equal to the pressure in the surrounding plenum.
7. The data for the solid wall marginally suggest that the maximum value of the drag coefficient during inflation was progressively greater than the interference-free  $C_D$  as model size increased. It is not known whether this behavior is the direct result of wall interference in the conventional sense or a consequence of the transient static pressure gradient.
8. Within measurement accuracy and subject to the the random nature of the inflation process, there was no discernible wall-interference effect on the peak  $C_D$  for any of the slotted-wall configurations.

#### References

1. Maskell, E. C., "A Theory of the Blockage Effects on Bluff Bodies and Stalled Wings in a Closed Wind Tunnel," Royal Aircraft Establishment Report No. Aero 2685, U.K., November 1963.
2. Macha, J. M. and Buffington, R. J., "Wall-Interference Corrections for Parachutes in a Closed Wind Tunnel," AIAA Paper No. 89-0900, ~~presented during the 10th Aerodynamic Decelerator Systems Technology Conference, Cocoa Beach, April 18-20, 1989.~~
3. Glauert, H., The Elements of Airfoil and Airscrew Theory, Cambridge University Press, Cambridge, 1948, Chapter XIV.
4. Rogers, E. W. E., "Wall Interference in Tunnels with Ventilated Walls," in AGARDograph 109, Subsonic Wind Tunnel Wall Correction, ed. by H. C. Garner, NATO-AGARD, Paris, October 1966, Chapter VI.

5. Barnwell, R. W., "Improvements in the Slotted-Wall Boundary Condition," in Proceedings, AIAA 9th Aerodynamic Testing Conference, 1976, pp. 21-30.
6. Everhart, J. L., "Theoretical and Experimental Studies of the Transonic Flow Field and Associated Boundary Conditions Near a Longitudinally-Slotted Wind-Tunnel Wall," Doctor of Science Dissertation, George Washington University, 1988.
7. Templin, J. T. and Raimondo, S., "Experimental Evaluation of Test Section Boundary Interference Effects in Road Vehicle Tests in Wind Tunnels," Journal of Wind Engineering and Industrial Aerodynamics, Vol. 22, 1986, pp. 129-148.
8. Holman, J. P. and Gajda, W. J., Experimental Methods for Engineers, 4th ed., McGraw-Hill, New York, 1984, Chapter 3.
9. Croll, R. H. et al, "Summary of Parachute Wind Tunnel Testing Methods at Sandia National Laboratories," AIAA Paper No. 81-1931, ~~presented during the~~ 7th Aerodynamic Decelerator and Balloon Technology Conference, San Diego, October 21-23, 1981.

#### DISCLAIMER

This report was prepared as an account of work sponsored by an agency of the United States Government. Neither the United States Government nor any agency thereof, nor any of their employees, makes any warranty, express or implied, or assumes any legal liability or responsibility for the accuracy, completeness, or usefulness of any information, apparatus, product, or process disclosed, or represents that its use would not infringe privately owned rights. Reference herein to any specific commercial product, process, or service by trade name, trademark, manufacturer, or otherwise does not necessarily constitute or imply its endorsement, recommendation, or favoring by the United States Government or any agency thereof. The views and opinions of authors expressed herein do not necessarily state or reflect those of the United States Government or any agency thereof.

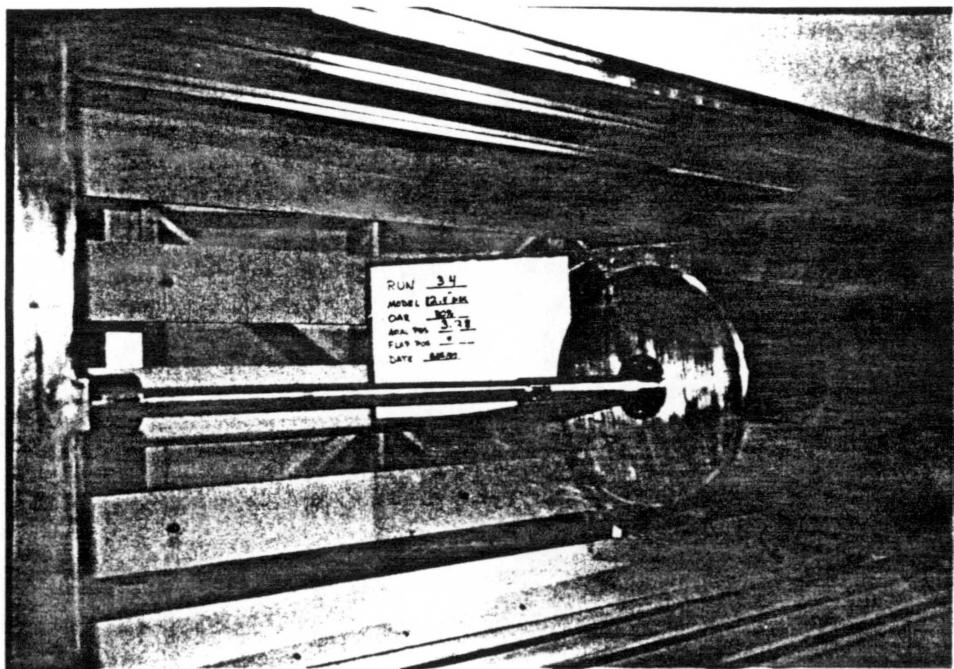


Fig. 1. Photograph showing the 0.15-GBR disk installed in the test section with the 0.3-OAR walls.

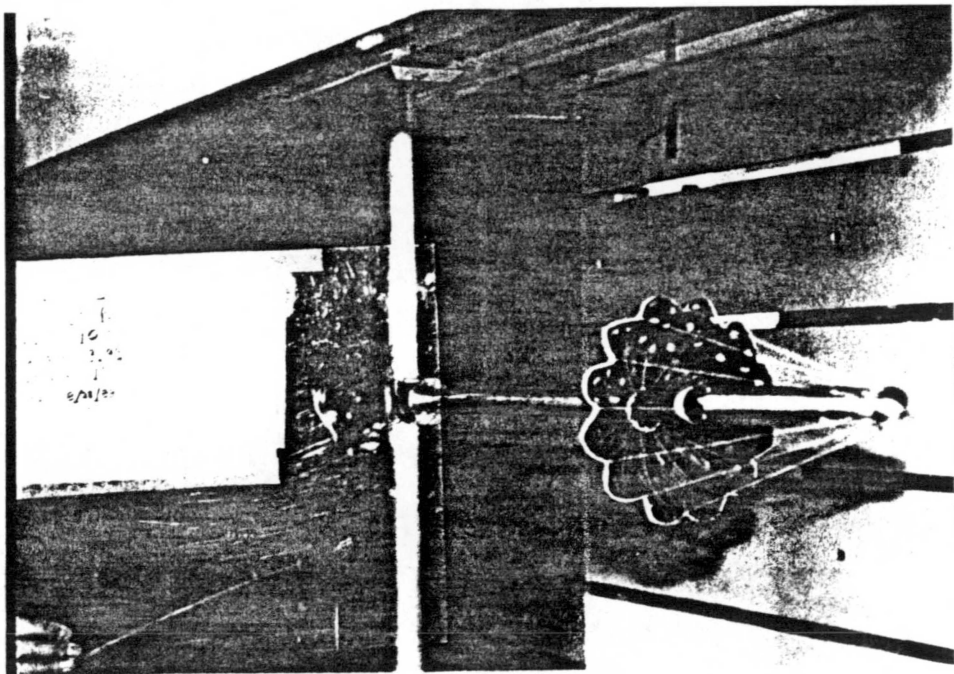


Fig. 2. Photograph showing the inflated 0.05-GBR parachute installed in the test section with the 0.1-OAR walls.

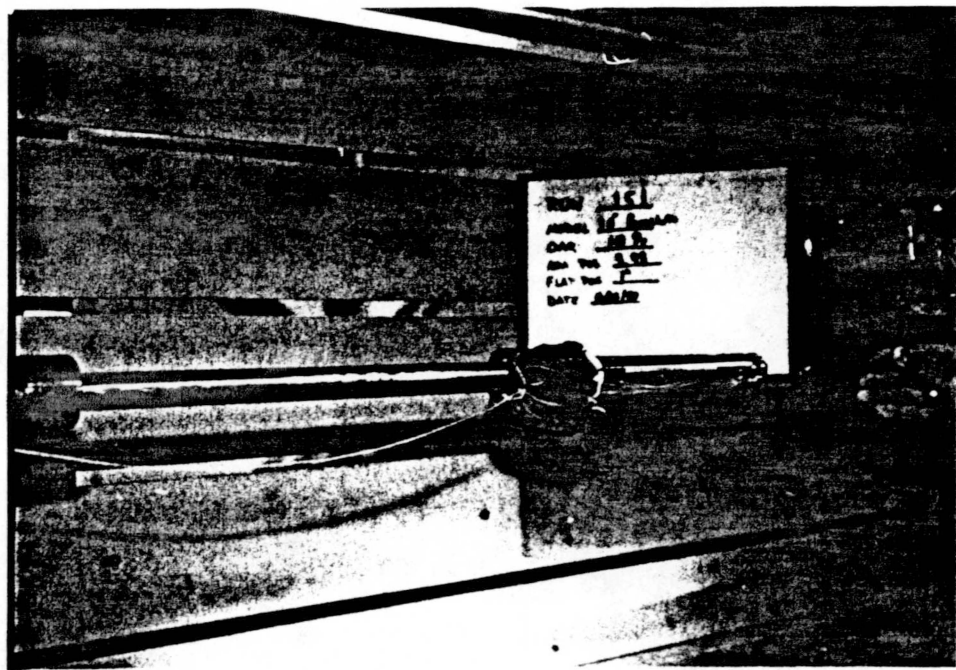


Fig. 3. Photograph showing the pre-inflation model configuration for the same run as depicted in Fig. 2.

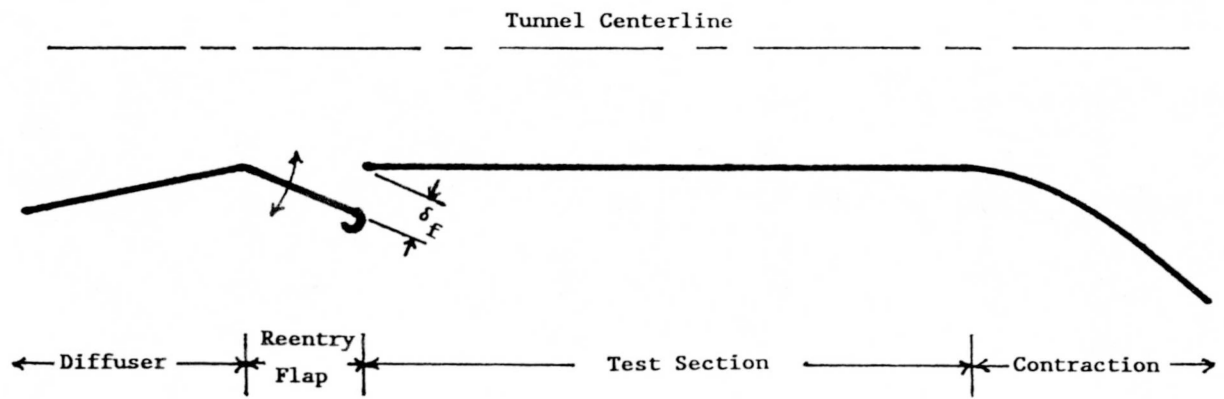
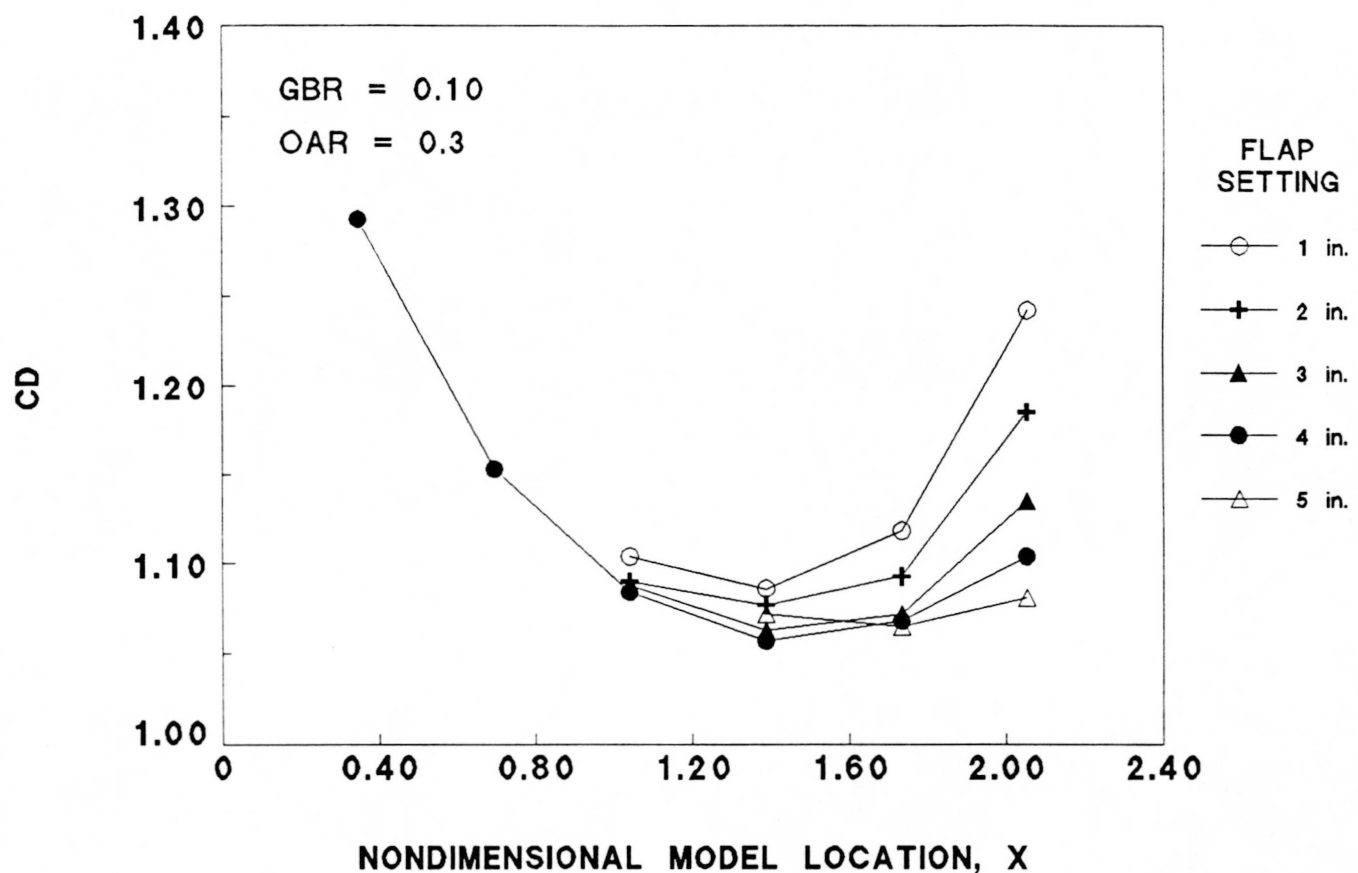


Fig. 4. Details of the diffuser reentry-flap geometry.



JMM:1024892

Fig. 5. Drag coefficient of the 0.10-GBR disk as a function of model location and reentry-flap setting for a wall open area ratio of 0.3.

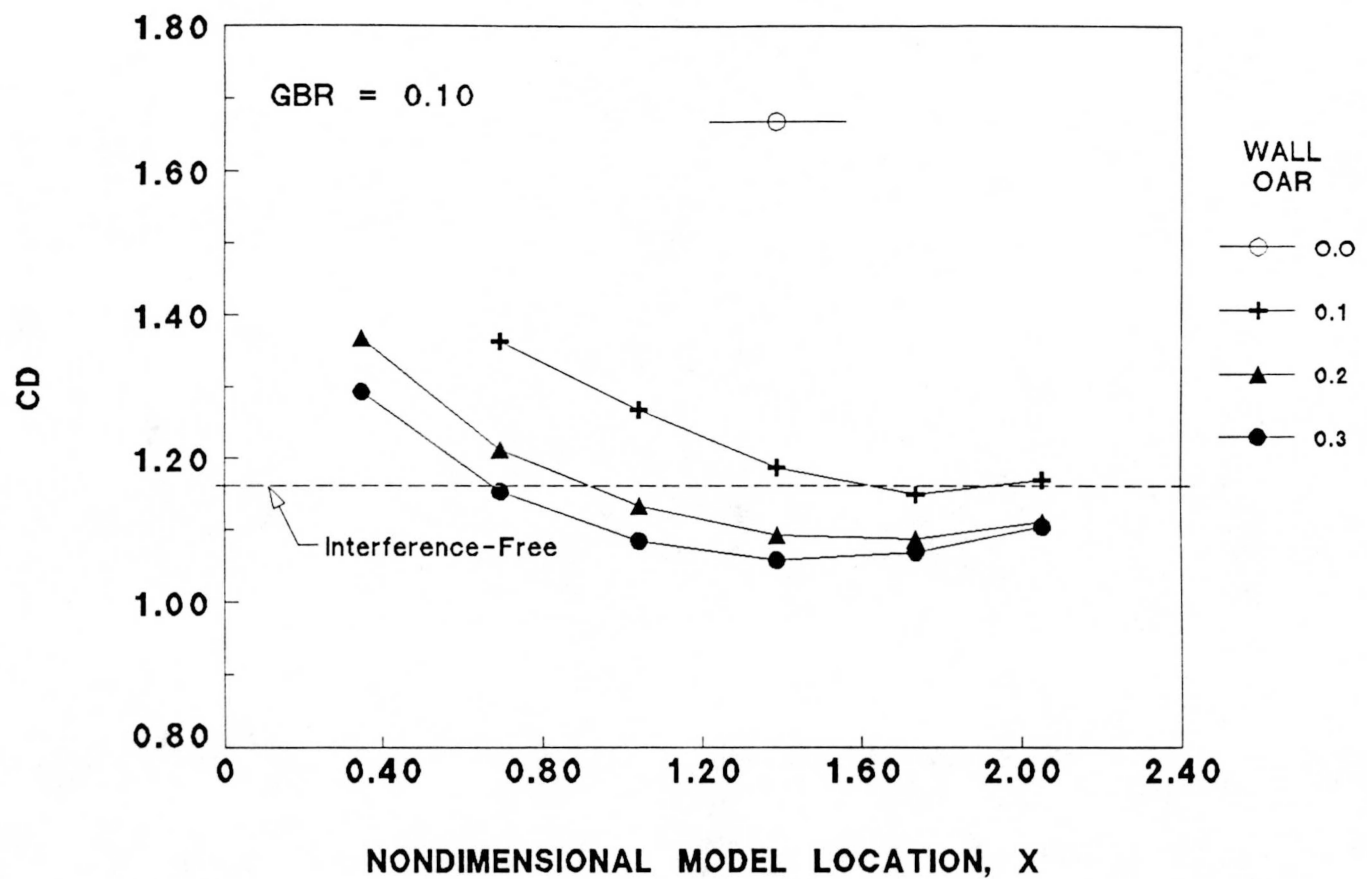
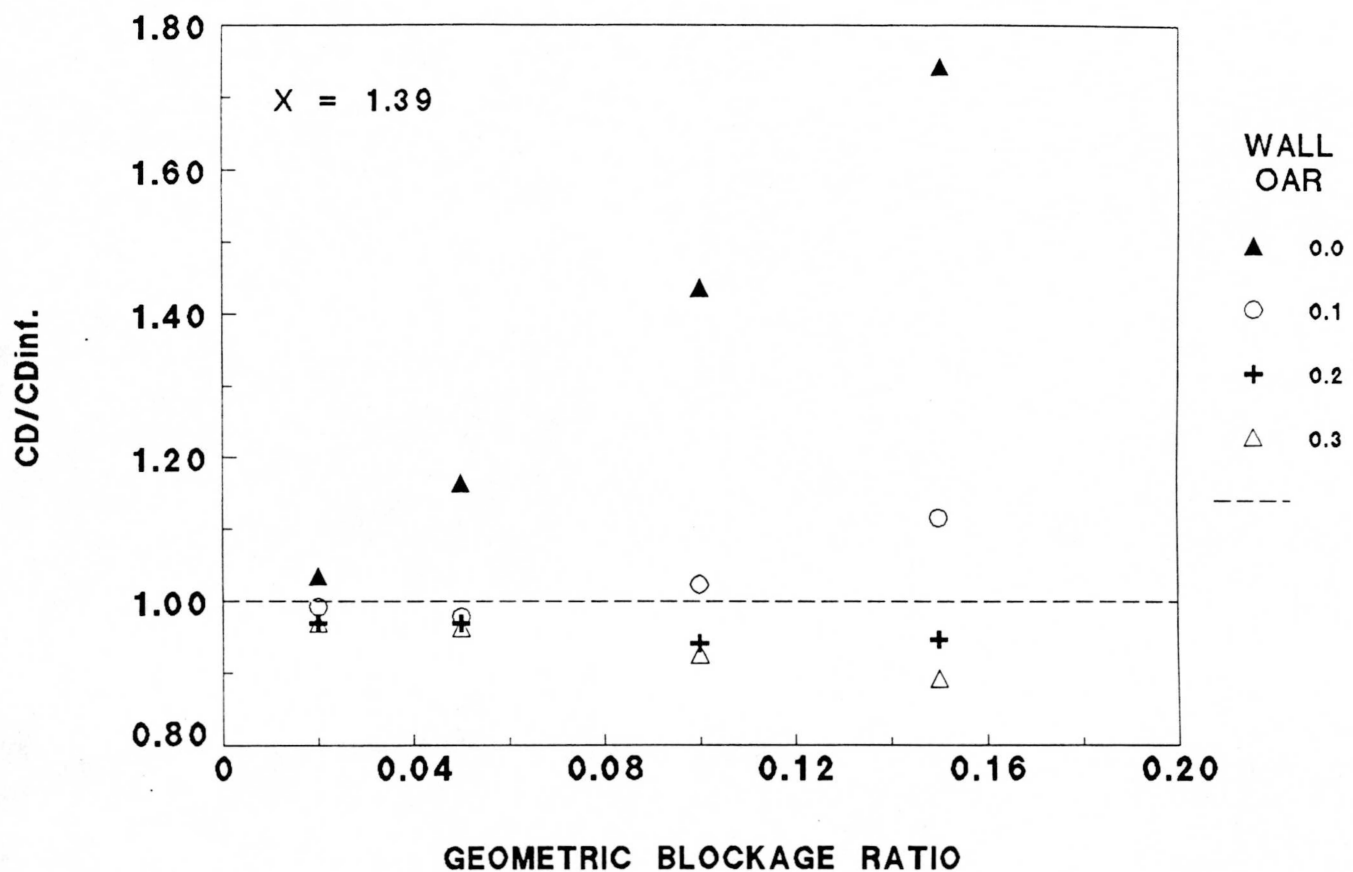


Fig. 6. Drag coefficient of the 0.10-GBR disk as a function of model location and wall OAR. ( $\delta_f = 4$  in.)

JMM:1025891



JMM:1024891

Fig. 7. Disk drag coefficient as a function of geometric blockage ratio and wall open area ratio. ( $X = 1.39$ )

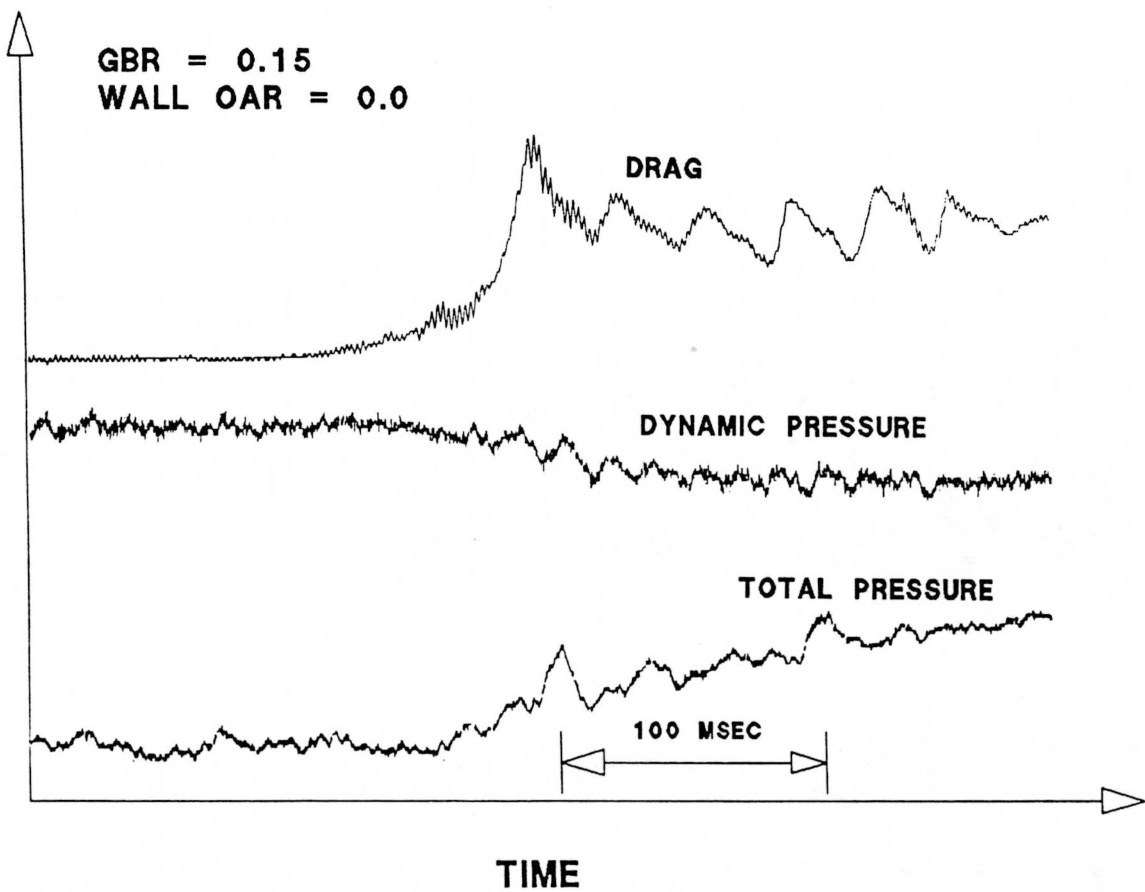


Fig. 8. Drag and test section airstream conditions during the inflation of the 0.15-GBR parachute with solid walls.

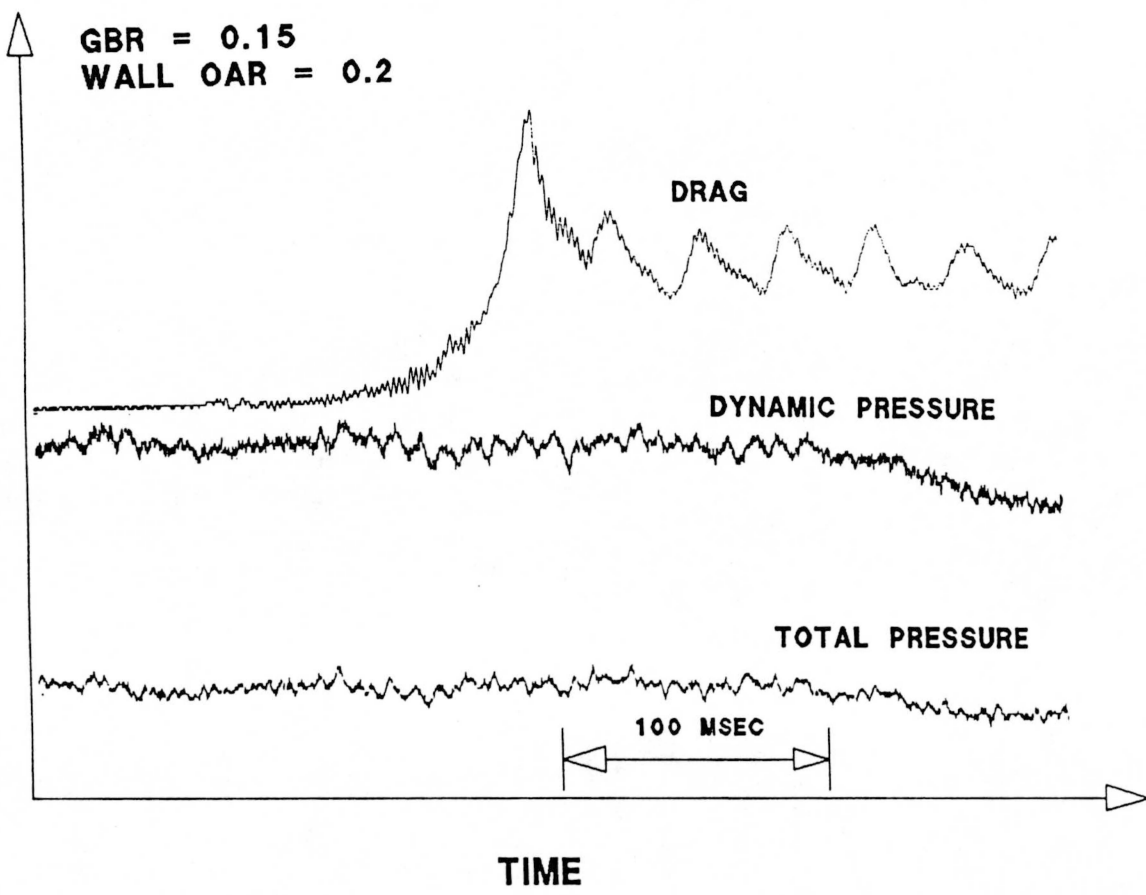
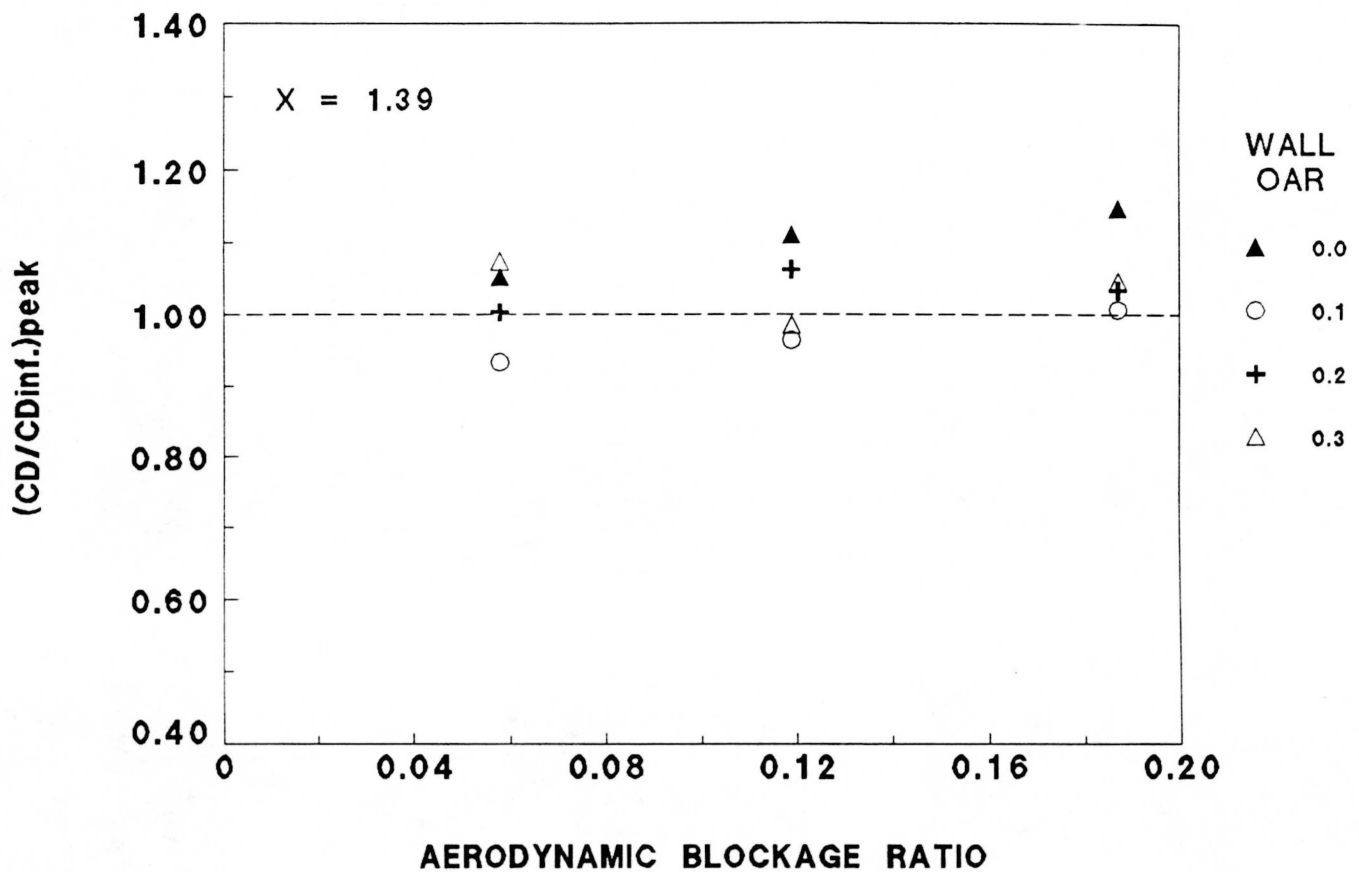


Fig. 9. Drag and test section airstream conditions during the inflation of the 0.15-GRB parachute with 0.2-OAR slotted-walls.



JMM:1025892

Fig. 10. Parachute peak drag coefficient as a function of model aerodynamic blockage ratio and wall open area ratio.